Title: N-acetyl-transferases required for iron uptake and aminoglycoside resistance promote virulence lipid production in *M. marinum*

Authors:

Bradley S. Jones[1,2], Vikram Pareek[1], Daniel D. Hu[3], Simon D. Weaver[3], Camille Syska[1,4], Grace Galfano[1], Matthew M. Champion[2,3], Patricia A. Champion[1,2]

[1]Department of Biological Sciences, [2]Eck Institute for Global Health, [3]Department of Chemistry and Biochemistry, University of Notre Dame, Notre Dame IN, 46556

[4]Current address: CNRS – CRBM, Montpellier, France

Abstract

Mycobacterial pathogens, including *M. tuberculosis,* the cause of human tuberculosis, and the non-tubercular species, *M. marinum* exhibit lytic activity in the host phagosome that is essential for disease. Acetylation is a conserved protein modification that is mediated enzymatically by N-acetyltransferases (NATs). NATs acetylate protein N^{α}-termini, lysine residues, and small molecules like antibiotics to alter bacterial physiology and pathogenesis. We sought to define conserved mycobacterial NATs required for lytic activity. We generated and characterized a library of *M. marinum* strains with deletions in predicted conserved NAT genes*. M. marinum* lyses red blood cells in a contact dependent manner. We screened our strains for hemolytic activity. We found that nearly all of the conserved lysine acetyltransferases (KATs) contributed to the hemolytic activity of *M. marinum*. Hemolysis is mediated by both the ESX-1 secretion system and by phthiocerol dimycocerosate (PDIM), and outer lipid required for virulence. We found that the hemolytic activity in several KAT deletion strains was restored by the addition of second copy of the ESX-1 locus. Using thin-layer chromatography (TLC), we found that MbtK was essential for PDIM and phenolic glycolipid (PGL) production. MbtK is a conserved KAT required for mycobactin siderophore synthesis and virulence. We found that the Δ*mbtK M. marinum* strain was attenuated

in macrophage and *Galleria mellonella* infection models. We show that the addition of Mycobactin J exogenously complements PDIM/PGL production in the *ΔmbtK* strain, linking production of these lipids to iron uptake. Constitutive expression of either *eis* or *papA5,* which encode a known KAT and a PDIM/PGL biosynthetic enzyme, rescued PDIM/PGL production and virulence of the Δ*mbtK* strain. Eis is an N-acetyltransferase linked to aminoglycoside resistance. We found that Eis N-terminally acetylated PapA5 *in vitro*, suggesting that Eis modification of PapA5 in the absence of MbtK restored lipid production. Overall, our study defines new connections between the MbtK and Eis NATs, and between iron uptake and PDIM and PGL synthesis in *M. marinum*. Moreover, out findings underscore the multifunctional nature of mycobacterial NATs and their connection to key virulence pathways.

Importance: Acetylation is a ubiquitous modification of protein N-termini, lysine residues, antibiotics and lipids. Many of the enzymes that promote acetylation belong to the GNAT family of proteins. *M. tuberculosis* is the causative agent of Tuberculosis. *M. marinum* is a related pathogen that is well established as a model to understand aspects of how *M. tuberculosis* causes disease. In this study we sought to identify conserved GNAT proteins required for early stages of mycobacterial infection. Using *M. marinum,* we determined that several GNAT proteins are required for the lytic activity of *M. marinum.* We uncovered previously unknown connections between acetyltransferases required for iron uptake and antimicrobial resistance, and the production of the unique mycobacterial lipids, PDIM and PGL. Importantly, our data support that acetyl-transferases from the GNAT family are interconnected, and have activities beyond those previously reported in the literature.

Introduction:

Acetylation is the movement of an acetyl group from an acetyl donor to an amine including N^{α}-amino groups (N-terminal acetylation), the ε-amine of lysine (N^{ε}-acetylation) or primary amines

53 of nucleotides, peptides, and small molecules (1). Acetylation can be facilitated enzymatically by
54 N-acetyltransferases (NATs). N-terminal protein acetylation is considered irreversible because N-
55 terminal deacetylases have not been identified. Lysine acetylation is reversible by lysine deacety-
56 lases (2-4) . Protein acetylation regulates protein folding, stability, localization, and protein-protein
57 interactions (5-11).

58 *Mycobacterium tuberculosis* is the cause of the human disease tuberculosis (12). In 2022,
59 *M. tuberculosis* infected 10.6 million individuals, resulting in an estimated 1.3 million deaths world-
60 wide (13). *M. marinum* causes a tuberculosis-like disease in poikilothermic fish, and is an occa-
61 sional human pathogen.

62 *M. marinum* serves as a model for several aspects of *M. tuberculosis* pathogenesis (14,
63 15). We previously reported the N-terminal acetylomes of *M. tuberculosis* and *M. marinum (16) .*
64 We found that 15% of *M. tuberculosis* proteins and 11% of *M. marinum* proteins are acetylated
65 at their N-termini (16). Approximately 16% of the mycobacterial proteome is acetylated at lysine
66 residues (17)**.** Acetylation mapped to metabolism, antibiotic resistance, iron uptake, and lipid syn-
67 thesis pathways critical to pathogenesis (17-20)**.**

68 The majority of predicted and established NATs belong to the GCN-5 Related N-acetyl-
69 transferase (GNAT) superfamily of enzymes (1). *M. tuberculosis* and *M. marinum* share 23 highly
70 conserved acetyltransferases (16), several of which are capable of acetylating more than one
71 type of target (21-31). Substrates of NATs cannot be predicted by protein sequence alone, requir-
72 ing that the substrates be determined empirically (*3*).

73 Early following infection, mycobacterial pathogens are taken up by professional phago-
74 cytes (32, 33). Following adaptation to the phagosome (34, 35), pathogenic mycobacteria use the
75 ESAT-6-system-1 (ESX-1) Type VII secretion system to lyse the phagosomal membrane and
76 promote interaction with the macrophage cytoplasm (36-40). Several mycobacterial lipids, includ-
77 ing phthiocerol dimycocerosate (PDIM) and phenolic glycolipid (PGL), promote optimal phagoso-
78 mal lysis (41-43), likely because these lipids are required for the wild-type levels of ESX-1 effector

79 proteins (44). Several ESX-1 proteins (EsxA, EspA, EspB, EspC, EspL, $EccA_1$, $EccB_1$, $EccCb_1$,
80 $EccE_1$, EsxH, and EspB), and PDIM/PGL biosynthesis proteins (Mas, PpsA, PpsE, Pks15/1,
81 PapA5 and DrrA) are N-terminally or lysine acetylated (16, 17, 45). We recently identified the
82 Emp1 (MMAR_1839) NAT as the sole enzyme that promotes N-terminal acetylation of EsxA in
83 *M. marinum in vivo (46)*. Here, we sought to identify highly conserved GNAT proteins between *M.*
84 *marinum* and *M. tuberculosis* that promote virulence through the ESX-1 and PDIM pathways,
85 leveraging genetics, biochemistry, proteomics, functional assays and models of infection.
86
87 **Results:**
88 **Several GNAT proteins contribute to *M. marinum* hemolytic activity***.* We generated *M. mari-*
89 *num* strains lacking individual genes with predicted or established NAT activity [Table 1, (46)],
90 and the corresponding complementation strains. We confirmed each strain using PCR (Figure
91 S1) followed by targeted DNA sequencing. ESX-1 and PDIM/PGL are required for optimal phag-
92 olytic activity of *Mycobacterium* (42, 47, 48). We tested the requirement of 19 conserved NATs
93 for *M. marinum* hemolytic activity, which can serve as a proxy for phagolytic activity. Six NATs
94 significantly impacted *M. marinum* hemolytic activity (Fig. 1A), while the remaining 13 NATs did
95 not significantly impact hemolysis (Fig. S2A). WT *M. marinum* lysed red blood cells (RBCs), while
96 the Δ$eccCb_1$ strain, which lacks a functional ESX-1 secretion system (37, 49), failed to lyse RBCs
97 (P<0.0001 relative to the WT strain) similar to the cell-free control (PBS). None of the *M. marinum*
98 strains lacking individual NATs phenocopied the Δ$eccCb_1$ strain (Figs. 1A and S2A). However,
99 the deletion of several individual NAT genes significantly reduced hemolysis compared to the WT
100 strain, including *argA, rimI*, *pat, MMAR_3205, MMAR_0332* and *mbtK* (all P<0.0001 vs the WT
101 strain*,* Fig. 1A). The *Δeis* strain was significantly more hemolytic than the WT strain (P=0.0032).
102 For all strains, except Δ*pat,* expression of the NAT gene of interest from the mycobacterial optimal
103 promoter significantly increased hemolysis compared to the deletion strain. From these data, we

104 conclude that several putative and established NATs are required for wild-type hemolytic activity
105 in *M. marinum.*

106 Several of the NATs were either established or predicted lysine acetyl transferases [KATs
107 in Fig 1A indicated by open bars, (21, 24, 26, 50-56)], and are the focus of this study. To test if
108 the predicted NAT impacted ESX-1 activity, we added an additional copy of the ESX-1 system to
109 the NAT deletion strains and tested for restoration of hemolysis. We introduced the pRD1-2F9
110 cosmid containing the extended RD1 locus from *M. tuberculosis*, which includes the majority of
111 the ESX-1 component and substrate genes (57), into the *M. marinum* strains lacking individual
112 KAT genes, as well as the WT and Δ$eccCb_1$ strains. The addition of a second copy of the ESX-1
113 locus to the WT strain did not significantly impact hemolysis (Fig. S2B). Because the $eccCb_{1MT}$
114 (MT = *M. tuberculosis*) gene is included on the pRD1-2F9 cosmid, the pRD1-2R9 plasmid com-
115 plemented the hemolytic activity of the Δ$eccCb_1$ strain. Interestingly, the pRD1-2F9 cosmid sig-
116 nificantly increased the hemolytic activity of the Δ*pat* and Δ*3205* strains (P<0.0001*,* relative to the
117 parent strains), supporting that Pat and MMAR_3205 impact hemolytic activity through the ESX-
118 1 system. The pRD1-2F9 cosmid did not significantly impact the hemolytic activity of the Δ*rimI,*
119 Δ*eis* or Δ*mbtK* strains, suggesting a specific connection between Pat and MMAR_3205*.*

120 We next tested if the deletion strains had altered production of PDIM, phenolic glycolipids
121 (PGLs) and tri-acyl glycerides (TAG). We extracted total lipids from the *M. marinum* strains lacking
122 individual KAT genes and their respective complementation strains and measured PGLs, PDIM
123 and TAG using TLC. The WT strain, but not the Δ*mas* strain produced PDIM, TAG (Fig. 1B, top
124 TLC) and PGL [bottom TLC, lane 1 and 2, (44, 46, 58-63)]. Both PDIM and PGL were reduced
125 and TAG levels were elevated in total lipids extracted from the Δ*mbtK* strain (lane 3). Expression
126 of the *mbtK* gene in the Δ*mbtK* strain increased PDIM and PGL, but did not reduce TAG levels
127 compared to the Δ*mbtK* strain (lane 4). Deletion or complementation of the other potential KAT
128 genes did not noticeably impact the lipids tested under these conditions (lanes 5-14). From these
129 data, we conclude that MbtK is required for the production of WT levels of PDIM and PGLs.

130

131 **Mycobactin deficiency is linked to reduced growth and PDIM and PGL production in *M.***
132 ***marinum.*** MbtK in is required for synthesizing mycobactin, a secreted siderophore required for
133 iron scavenging (55). In the absence of MbtK, *M. tuberculosis* growth *in vitro* was severely im-
134 pacted due to the loss of mycobactin production (55). Likewise, we found that the *ΔmbtK* strain
135 exhibited significantly reduced growth compared to the WT and complemented strains (Fig. S3A).
136 We next tested if the reduced growth and PDIM production in the Δ*mbtK M. marinum* strain could
137 be rescued by supplementing the Δ*mbtK* strain with ferric Mycobactin J. As shown in Figure S3C,
138 addition of mycobactin to the growth media restored growth of the Δ*mbtK* strain, similar to the
139 complemented and WT strains. We grew the *M. marinum* strains in the presence of a range of
140 mycobactin concentrations (from 2 µg/ml to 0.0002 µg/ml or in the absence of mycobactin) and
141 extracted total lipids. Using TLC, we found that PDIM and PGL production was restored to WT
142 levels in the presence of 2 µg/ml or 0.02 µg/ml mycobactin (Fig. S3C). 0.0002 µg/ml did not restore
143 PDIM or PGL production to the Δ*mbtK* strain From these data we conclude that the addition of
144 mycobactin J to the grown media trans-complemented the growth defect and PDIM/PGL produc-
145 tion of the Δ*mbtK* strain. These data support the idea that PDIM and PGL production was reduced
146 in the Δ*mbtK* strain due to a deficiency in iron scavenging.

147 MbtK, and its role in mycobactin synthesis, was previously linked to phospholipid homeo-
148 stasis (55). However, MbtK has not previously been linked to PDIM and PGL production. To gain
149 insight into the mechanisms underlying the phenotypes associated with the loss of MbtK we used
150 proteomics to measure the changes in protein levels. We generated cell-associated and secreted
151 protein fractions from the WT, Δ*mbtK,* and the Δ*mbtK*/p*mbtK* strains (Dataset S1) and measured
152 protein levels in each fraction using nUHPLC MS-MS/MS quantitative bottom-up proteomics (44,
153 64). The deletion of *mbtK* resulted in a significant increase in 15 proteins (Figure S4A), the ma-
154 jority of which are associated with three chromosomal regions associated with iron uptake, includ-
155 ing ESX-3 (EccB3 and MycP3), MMAR_2874, MMAR_2875, cyp278A1 and MMAR_2878, which

156 are colocalized on the chromosome, and MbtF, MbtE and MbtD, which are colocalized with MbtK
157 on the chromosome. The Cyp278A1 protein is annotated as being involved in heme uptake (65).
158 The additional genes are conserved hypothetical proteins. Expression of *mbtK* in the Δ*mbtK* strain
159 restored protein levels to those in the WT strain. We also measured the protein levels in the
160 secreted fractions. The levels of the Mbt proteins were increased in the secreted fraction from the
161 Δ*mbtK* strain as compared to the strains expressing *mbtK*. There was no significant change in
162 the secretion of any ESX proteins to explain the reduced hemolytic activity in Fig. 1A. These data
163 did not allow us to connect the loss of MbtK to the production of PDIM and PGL.
164
165 **Overexpression of *eis* restores virulence lipids to the Δ*mbtK* strain.** To understand the re-
166 quirement for MbtK in the lipid biosynthesis, we asked if constitutive expression of the other pu-
167 tative KAT genes could restore wild-type PDIM, PGL and TAG levels to the Δ*mbtK* strain. We
168 introduced each KAT gene into the Δ*mbtK* strain on an integrating plasmid, expressed from the
169 MOP promoter, and confirmed the presence of the plasmid in each strain by PCR (Fig. S5). The
170 expression of the *riml, pat* or *MMAR_3205* genes did not detectably impact the levels of PDIM,
171 TAG or PGLs in the Δ*mbtK* strain (Fig. 2A, lanes 5-7). However, constitutive expression of the
172 *eis* gene specifically restored PDIM, TAG and PGL levels in the Δ*mbtK* strain (lane 8) to those in
173 the WT and complemented strains.
174 Eis is a N-acetyltransferase that is clinically linked to aminoglycoside resistance in *M. tu-*
175 *berculosis* (28, 66-71). To our knowledge, there are no known connections between the Eis and
176 MbtK acetyltransferases. We first considered if Eis restored lipid production simply because it was
177 the most similar NAT to MbtK. Based on structural predictions, MbtK and Eis proteins do not share
178 domains beyond the conserved GNAT domains (AlphaFold, Fig 2B). The RimI, Pat or
179 MMAR_3205 proteins that did not functionally complement the Δ*mbtK* also share the GNAT do-
180 main. At the amino acid level, Eis, RimI and MMAR_3205 are all ~20% identical to MbtK (Fig.
181 2C), and both MbtK1 and MMAR_3205 are more phylogenetically related KAT to MbtK the Eis

182 (Fig. 2D). Therefore, we hypothesized that Eis specifically restored PDIM/PGL production to the
183 Δ*mbtK* strain. Our proteomics analysis shows that expression of *eis* in the Δ*mbtK* strain restored
184 the levels of 12 of the 15 previously discussed proteins, with the exception of MMAR_2874,
185 MMAR_2875 and Cyp278A1, which are at the same genetic locus (Fig. S4). These data suggest
186 that *eis* partially complements the Δ*mbtK* strain.

187 *M. tuberculosis* required supplementation with iron during laboratory culture when the
188 $mbtK_{MT}$ gene was deleted (55). The Δ*mbtK* (*MMAR_3692*) *M. marinum* strain exhibited reduced
189 growth without the addition of supplemental iron compared to the WT strain (Fig. S3A). An ortho-
190 logous *mbtK* gene, *MMAR_1587*, in *M. marinum* genome which may allow growth of the Δ*mbtK*
191 strain without additional iron. MMAR_1587 is 28.5% identical at the amino acid level, and is pre-
192 dicted to be structurally similar to MbtK (Fig. S6A) MMAR_1587 is 54.73% identical to the $MbtK_{MT}$
193 protein at the amino acid level, and is annotated as the MbtK ortholog on Mycobrowser (15).
194 Although the MMAR_3692 protein is 26% identical to $MbtK_{MT}$, the *MMAR_3692* gene is syntenic
195 with the $mbtK_{MT}$. As such, we refer to *MMAR_3692* as *mbtK,* and *MMAR_1587* as *mbtK1.* (Fig.
196 2D). *M. marinum* has an orthologous *eis* gene, *MMAR_0151,* which is annotated as *eis1* (65).
197 The Eis and Eis1 proteins are 31.44% identical, and are predicted to be structurally similar (Fig.
198 S6A). To further probe the interaction between MbtK and Eis, we constitutively expressed *mbtK1*
199 and *eis1* in the Δ*mbtK* strain. Constitutive expression of the *mbtK1* or *eis1* genes did not com-
200 pletely rescue PDIM or PGL levels in the Δ*mbtK* strain as visualized by TLC (Fig. S6B). These
201 data suggest that additional copies of MbtK or Eis are functionally redundant, and that Eis likely
202 specifically rescues PDIM, PGL and TAG production in the Δ*mbtK* strain.

203

204 **Eis N-terminally acetylates PapA5 *in vitro*.** The proteomics data did not provide an obvious
205 mechanism for how Eis restored PDIM and PGL production to the Δ*mbtK* strain. We demonstrated
206 that several proteins required for PDIM and/ or PGL production (PpsA, PapA5, Mas and PpsE,
207 Pks15/1) were N-terminally acetylated [Fig S7, Pink, (*1*)]. Although neither MbtK nor Eis have

208 reported to N-terminally acetylate proteins, we tested if MbtK and/or Eis could N-terminally acet-
209 ylate one or more biosynthetic proteins required for PDIM and PGL production.

210 It was previously established that the first six amino acids of a substrate protein were
211 sufficient for N-terminal acetylation *in vitro* (30, 72). We had N-terminal six AA peptides synthe-
212 sized based on the N-terminal peptides we previously measured using proteomics [Fig. 3A, (16)].
213 Only the Mas peptide contained a "K" residue, suggesting that we could measure N-terminal acet-
214 ylation of these peptides. The N-terminal peptides were used as substrates for *in vitro* acetylation
215 assays with the WT or inactive versions of MbtK (MbtKE161A, active site mutation as predicted
216 by UniProt) and Eis [EisY128A, proton donor active site mutant based on (29)] that we expressed
217 and purified from *E. coli* (Fig. S8). Transferring the acetyl group from Acetyl-CoA to a peptide
218 substrate results in a free thiol group on the resulting CoA molecule. The reaction of this free thiol
219 with 5, 5'-dithiobis-(2-nitrobenzoic acid) DTNB results in a colorimetric change that can be meas-
220 ured at 412nm. The resulting product has 1:1 stoichiometry with the acetylated peptide and can
221 be used to quantify protein acetylation (29, 73). The RimI NAT from *Salmonella* with the S18
222 substrate [(72, 74), Fig. S8] was a positive control for the reaction. Incubation of the PpsE
223 (P=0.0147) or PapA5 (P<0.0001) peptides with the WT MbtK resulted in significantly higher DTNB
224 production than incubation with the MbtKE161A protein (Fig. 3B). Incubation of the PpsA, Mas or
225 Pks15/1 peptides resulted in product formation that was not significantly different between the
226 active and inactive enzymes. These data support that MbtK may acetylate the N-terminal amino
227 acid of PpsE or PapA5.

228 We conducted the same experiment using Eis or EisY128A, a proton donor active site
229 mutant (29). Incubation of the PapA5 peptide with the WT Eis protein resulted in significantly
230 higher DTNB production than incubation with the Eis Y128A protein (P=0.0096, Fig. 3C). None of
231 the other peptides tested exhibited significantly reduced product formation between the WT and
232 dead enzymes. These data are consistent with the possibility that Eis may N-terminally acetylate
233 PapA5.

234 To directly test the acetylation of PpsE and PapA5 by MbtK and Eis, we used FIA mass
235 spectrometry. As shown in Figure 3D, MbtK did not N-terminally acetylate the PpsE peptide. Alt-
236 hough we detected the unacetylated peptide (left), we did not detect the acetylated peptide. We
237 likewise tested if Eis or MbtK could N-terminally acetylate the PapA5 peptide. The unacetylated
238 PapA5 peptide was detected when mixed with either Eis (Fig. 3E, top left) or MbtK (bottom left).
239 The acetylated PapA5 peptide was detected in the presence of Eis, but not MbtK (Fig. 3E, right).
240 We conclude that Eis, but not MbtK, N-terminally acetylates PapA5 *in vitro*. These data suggest
241 that *eis* expression in the Δ*mbtK* strain restores PDIM production by N-terminal acetylation of the
242 PapA5 protein (Fig. 3F). We attempted to measure N-terminal acetylation in the Δ*mbtK* strain,
243 and in the corresponding complementation and *eis* expression strain (Dataset S1). We were un-
244 able to measure the N-terminal peptide of PapA5 in these strains. We did not identify N-terminal
245 peptides whose acetylation in the Δ*mbtK* strain was significantly decreased and was restored by
246 both the *mbtK* and *eis* expression, or by expression of the *eis* gene. Potential candidates for
247 targets that did not reach significance are in (Fig. S4B). These data did not allow us to determine
248 if the N-terminal acetylation of PapA5 was promoted by *eis* expression in *M. marinum*.

249 We tested if *papA5* could restore PDIM/PGL production or growth to the *ΔmbtK* strain by
250 collecting total lipids and visualizing PDIM and PGL on TLCs. Expression of *papA5* did not in-
251 crease PDIM or PGL Levels (Fig. 3F, lanes 2 and 3). Expression of the *papA5* gene in the Δ*mbtK*
252 strain increased the levels of PDIM and PGLs in this strain, but not to WT levels (lanes 4 and 5,
253 and additional replicates in Fig S9). Together these data support the conclusion that although
254 PapA5 partially rescued the reduced PDIM/PGL levels in the Δ*mbtK* strain, it did not rescue
255 growth under the conditions tested.

256 **The requirement of MbtK for mycobacterial pathogenesis can be suppressed by Eis**
257 **or PapA5.** Because the Δ$mbtK_{MT}$ was attenuated for virulence in a mouse model of infection (55),
258 we tested if the Δ*mbtK* strain was attenuated in two models of mycobacterial infection. First, we
259 tested if *mbtK* was required for macrophage cytolysis using Ethidium homodimer (Eth-D1), which

260 is a membrane impermeable nucleic acid stain (*16*). If *M. marinum* infection perforates the mac-
261 rophage membrane, the cells stain red. We infected RAW 264.7 cells with *M. marinum* at an M
262 OI of 5, and counted the presence of red cells (Fig. 4A). Infection of RAW 264.7 cells with wild-
263 type *M. marinum* (P<0.0001), but not the Δ*eccCb*$_1$ strain, resulted in significant levels of cytolysis
264 compared to the uninfected cells. The Δ*mas* strain and the Δ*mbtK* strains resulted in significantly
265 less cytolysis than the WT strain (P<0.0001). The complementation strains significantly increased
266 cytolysis compared to the deletion strains (P<0.0001) but were still significantly lower than the
267 WT strain (P<0.0001and P=0.0090, respectively). The *ΔmbtK* strain expressing the *mbtKE161A*
268 gene did not significantly affect cytolysis compared to the Δ*mbtK* strain. From these data we con-
269 clude that the NAT activity of MbtK is required for macrophage cytolysis.

270 We tested macrophage cytolysis following infection with the Δ*mbtK* strain constitutively
271 expressing the *eis* or the *eisY128A* gene (Fig. 4B). Expression of the *eis* or *eisY128A* gene in the
272 Δ*mbtK* strain significantly increased cytolysis compared to the Δ*mbtK* strain (P<0.0001), similar
273 to the WT strain. Infection with the Δ*mbtK* strain expressing the *eisY128A* gene resulted in signif-
274 icantly reduced cytolysis compared to the *eis* gene (P=0.0001). We conclude that constitutive
275 expression of *eis* suppresses the loss of MbtK during macrophage infection, and that this sup-
276 pression requires the NAT activity of Eis.

277 We tested if constitutive expression of *papA5* would likewise restore cytolysis to the Δ*mbtK*
278 strain. Infection of RAW 264.7 cells with the Δ*mbtK* strain constitutively expressing *papA5* resulted
279 in significantly more cytolysis than the WT (P=0.0218) or Δ*mbtK* strains (P<0.0001, Fig. 4A). To
280 test if suppression of cytolysis by *papA5* expression was specific we added two controls. First,
281 constitutive expression of *papA5* in the Δ*mas* strain failed to restore cytolysis to the Δ*mas* strain.
282 Second, constitutive expression of the *rimI* NAT in the Δ*mbtK* strain failed to restore cytolysis to
283 the Δ*mbtK* strain. Collectively, our data support that acetylation of PapA5 by Eis bypasses the
284 loss of MbtK.
285

286 We tested if the orthologous *mbtK1* and *eis1* genes were essential for macrophage cytol-
287 ysis. Expression of the *mbtK1* gene partially restored cytolysis to the Δ*mbtK* strain (Fig. S7B)
288 Expression of the *eis1* gene in the Δ*mbtK* strain resulted in cytolysis levels significantly higher
289 than the WT strain (P<0.0001). Deletion of the *mbtK1* or *eis* genes significantly reduced macro-
290 phage cytolysis compared to the WT strain (P<0.0001), but cytolysis was not restored upon ex-
291 pression of *mbtK1* or *eis* in these strains. Deletion of the *eis1* gene resulted in a significant reduc-
292 tion of macrophage cytolysis compared to the WT strain, and this was significantly increased upon
293 expression of the *eis1* gene, though not to WT levels.

294 To complement the cellular model of infection, we tested the ability of *M. marinum* to kill
295 the waxworm, *Galleria mellonella* larvae*. G. mellonella* was previously established as a model for
296 mycobacterial infection (75-79). For each experiment, we infected 30 worms, each injected with
297 $1x10^7$ bacteria in a 5 µL volume. Experiments were performed in biological triplicate. As shown in
298 Figure 4B, WT *M. marinum* killed all of the infected *G. mellonella* by 7 days post-infection. In
299 contrast, infection with either the Δ*eccCb*$_1$ or Δ*mbtK* strains resulted in less killing, similar to the
300 uninfected worms. Deletion of *eis* did not significantly impact the killing of *G. mellonella.* Expres-
301 sion of *mbtK* restored the ability of the Δ*mbtK* strain to kill *G. mellonella,* similar to the WT strain.
302 Expression of either *eis* or *papA5* in the Δ*mbtK* strain partially restored the ability of *M. marinum*
303 to kill *G. mellonella.* Introduction of the pRD1-2F9 plasmid to the Δ*mbtK* strain or growing the
304 Δ*mbtK* strain in ferric mycobactin did not restore *G. mellonella* killing to the ΔmbtK strain (Fig.
305 S3B). Together, these data support that the expression of Eis or PapA5 suppresses the loss of
306 *mbtK* in *M. marinum.*

307

308 **Discussion:**

309 We sought to identify conserved GNAT containing proteins important for the ESX-1 and PDIM
310 virulence pathways. We found that the majority of GNAT proteins previously annotated as lysine
311 acetyltransferases were required for wild-type levels of hemolysis by *M. marinum.* We identified

312 several potential NATs required for hemolysis that could be rescued by the addition of a second
313 ESX-1 locus. These GNAT proteins will be followed up in future studies. Our data support a model
314 where mycobactin-mediated iron uptake promotes the PapA5-mediated biosynthesis of PDIM and
315 PGLs (80). In the absence of MbtK, the production of PDIM and PGLs is reduced compared to
316 the WT *M. marinum* strain. PDIM and PGL production was complemented by expression of either
317 *mbtK* or *in trans* by the addition of Mycobactin J to the growth media. Complementation was
318 dependent upon the acetyltransferase activity of MbtK, as expression of the *mbtKE161A* allele,
319 which does not have NAT activity, did not restore PDIM and PGL production. We showed that the
320 expression of *papA5* or the *eis* NAT in the Δ*mbtK* strain specifically suppressed the requirement
321 of MbtK in PDIM and PGL production. The simplest mechanism, which is supported by our *in vitro*
322 assays, is that Eis N-terminally acetylates PapA5, promoting the production of PDIM and PGL in
323 the absence of MbtK. Overall, our studies support a previously undiscovered link between MbtK,
324 iron uptake and the final step of PDIM and PGL biosynthesis (Fig. 5).

325 Our model is supported by several lines of evidence previously published in the literature.
326 It was previously established by Madigan et al that MbtK is required broadly for lipid and myco-
327 bactin production (55). MbtK is required for the synthesis of the lipid tail of the mycobactin sider-
328 ophore, but more broadly, the loss of MbtK and iron uptake in *M. tuberculosis* resulted in a deple-
329 tion of phospholipids during iron starvation (55). Although Madigan et al connected lipid produc-
330 tion to MbtK mediated siderophore iron uptake in *M. tuberculosis,* the PDIM and PGL lipids were
331 not readily measured using lipidomics approaches in this study. As such, the connection between
332 mycobactin dependent iron uptake and PDIM/PGL biosynthesis has not been previously investi-
333 gated. The connection between iron and PDIM/PGL biosynthesis could be direct. For example,
334 the PapA5 mediated synthesis step in PDIM biosynthesis could require iron. In support of this,
335 *papA5* overexpression or the addition of mycobactin restored PDIM/PGL biosynthesis in the
336 Δ*mbtK* strain. Alternatively, the connection between iron and PDIM/PGL biosynthesis could be
337 indirect. For example, it is possible that iron levels are a signal that regulate the production of

338 PDIM and PGL. Further experimentation is required to differentiate between these two possibili-
339 ties.

340 The mechanisms connecting MbtK to mycobacterial pathogenesis are unclear. Yet, it was
341 surprising that constitutive expression of the *papA5* or *eis* genes fully restored macrophage cytol-
342 ysis to the Δ*mbtK* strain. Infection of *G. mellonella* revealed that increasing PapA5 or Eis restored
343 virulence to the Δ*mbtK* strain, but the kinetics of killing differed from that of the WT strain. These
344 data support that perhaps expression of these genes restored PDIM/PGL production, but did not
345 fully complement the Δ*mbtK* strain. Further work is required to determine if constitutive expression
346 of *eis* or *papA5* restore more that the PDIM/PGL deficiency to the Δ*mbtK* strain.

347 In this study, we uncovered a link between Eis and PapA5. Eis is a bifunctional N-acetyl-
348 transferase that acetylates aminoglycoside antibiotics to inactivate them. Mutations that lead to
349 *eis* overexpression naturally occur in clinical isolates of *M. tuberculosis,* leading to kanamycin
350 resistance (28, 66-71). Numerous studies have reported inhibitors of Eis as a potential path to
351 prevent aminoglycoside resistance during *M. tuberculosis* infection (81-90). Eis reversibly acety-
352 lates lysine residues in the HupB protein, affecting chromosomal condensation in *M. tuberculosis*
353 (26). We showed that Eis N-terminally acetylates PapA5 *in vitro*, adding another potential activity
354 to this enzyme. We were unable to detect the N-terminal peptide of PapA5 in our proteomics
355 experiment. However, expression of *papA5* suppressed several phenotypes of the Δ*mbtK* strain
356 supporting this connection (Fig. 5). If Eis acetylates the N-terminus of PapA5 *in vivo*, this modifi-
357 cation must promote PapA5 activity, allowing suppression of the PDIM/PGL defect in the Δ*mbtK*
358 strain. Our data further support an emerging literature that NATs, including Eis, are multifunctional
359 (91).

360 Knobloch et al previously suggested that the orphan *mbtK* gene (*MMAR_1587*) was the
361 *M. marinum* ortholog of *M. tuberculosis* MbtK (92). Despite being located at the *mbt* locus,
362 *MMAR_3692* was not mentioned in this publication. In our study, we found that deletion of the
363 *MMAR_3692* gene resulted in reduced growth during standard culturing conditions. The growth

364 defect was significant, but unlike in *M. tuberculosis,* the deletion of *mbtK* did not abrogate growth.
365 Similar to *M. tuberculosis,* supplementation with mycobactin restored growth of the Δ*mbtK* strain
366 (55). Deletion of the *mbtK* gene, but not the *MMAR_1587* gene resulted in a measurable
367 PDIM/PGL defect. Likewise, expression of *MMAR_1587* in the Δ*mbtK* strain did not restore PDIM
368 levels. From our studies, we propose that the *MMAR_3692* gene is the *M. marinum* ortholog of
369 the *M. tuberculosis mbtK*. Our data also suggests that the two genes in *M. marinum* are function-
370 ally distinct.

371 In non-tubercular mycobacterial species, there are two functionally distinct eis genes. In
372 *M. abscessus,* these are annotated as Eis1Mab and Eis2mab (93). Overexpression of *eis2mab,*
373 but not *eis1mab,* resulted in resistance to Kanamycin. We likewise found that there are two po-
374 tential *eis* genes in *M. marinum.* Deletion of either *eis* gene attenuated *M. marinum* in a macro-
375 phage model of infection (Fig. S6C). Overexpression of *eis,* but not *eis1* in *M. marinum* resulted
376 in low level Kan resistance (Fig S10), supporting that robust literature linking Eis levels to amino-
377 glycoside resistance, and that the two *eis* genes are functionally distinct. Our macrophage infec-
378 tion data supports that overexpression of *eis1* restored cytolysis of the Δ*mbtK* strain to greater
379 than WT levels (Fig. S6). Yet, expression of *eis1* did not restore PDIM/PGL production to the
380 Δ*mbtK* strain. The mechanisms connecting Eis1 to MbtK need further experimentation.

381 Overall, this study revealed a new connection between iron scavenging and PDIM and
382 PGL biosynthesis that requires further investigation. We uncovered that the Eis NAT, which has
383 been widely linked to drug resistance in *Mycobacterium,* also has the potential to N-terminally
384 acetylate proteins, including those required for the production of the PDIM and PGL lipids. Our
385 data support that NATs cannot be characterized by the targets they modify, and likely play unex-
386 pected, interconnected and as of yet undefined roles in mycobacterial pathogenesis and physiol-
387 ogy.
388

389 **Methods:** A summary of the methods are found here. Where necessary, detailed methods are
390 provided in the Supplementary Information. *Mycobacterium marinum* strains were derived from
391 the *Mycobacterium marinum* M strain (ATCC BAA-535), and maintained as described previously.
392 In frame deletion strains were generated using allelic exchange, and can be found in TableS1.
393 Complementation plasmids, found in Table S2, were constructed using the primers in Table S3
394 using FastCloning. Site directed mutagenesis was performed as described previously (94). He-
395 molysis assays were performed as described. RAW 264.7 cells were maintained as described
396 and infected with *M. marinum* at an MOI of 5. Macrophage cytotoxicity were measured by meas-
397 uring Ethidium homodimer uptake as described. *G. mellonella* larval infections were performed
398 by injecting *M. marinum* at a concentration$1x10^7$/5µL. Thin-layer chromatography experiments
399 was performed as described in (46). Expression and purification of 6xHis-tagged proteins were
400 expressed in *E. coli,* and purified using Ni-NTA resin, followed by removal of the epitope tag using
401 TEV. Proteins were used to test activity in vitro against N-terminal peptides (Genscript) using 5,5-
402 dithio-bis-(2-nitrobenzoic acid) (DTNB) assays as (73) with minor modifications. Peptide acetyla-
403 tion following the DTNB assay was confirmed using MALDI. Bottom-up proteomics was performed
404 after labelling samples with deuterated acetyl groups as (16) to quantify protein levels and N-
405 terminal acetylation. Label-free quantification (LFQ) was used for differential protein expression
406 analysis, and data were processed using R (v4.3.2). The code can be found on github
407 (https://github.com/Champion-Lab/3692). Rawdata is available through MassIVE and The Prote-
408 ome Exchange at ftp://MSV000095200@massive.ucsd.edu with Identifier MSV000095200
409 PXD053528.

410 **Acknowledgements** We would like to thank Bill Boggess at the Notre Dame Mass Spectrometry
411 and Proteomics Facility for continued assistance. Research reported in this publication was sup-
412 ported by NIAID of the National Institutes of Health under award number AI106872. BSJ was
413 supported by a Graduate Fellowship from the Eck Institute for Global Health at the University of

Notre Dame. We thank Dr. Micah Ferrell, who constructed several NAT deletion strains used in Figure S1, during his training at Notre Dame.

Figure Legends

Figure 1. At least four Lysine acetyltransferases are required for WT levels of hemolytic activity in *M. marinum.* A. Hemolytic activity of *M. marinum* strains lacking genes encoding predicted NATs. The putative/ known KATs are not filled. -, + refers to absence or presence of complementation plasmid, which gene of interest expressed from the mycobacterial optimal promoter. Significance relative to the WT strain; Brackets report significance between the deletion and complemented strains. **** $P<0.0001$, *** $P=0.0004$, 0.0002, * $P=0.0250$, 0.0298, ** $P=0.0032$ **B.** TLC analysis of total lipids from the indicated *M. marinum* strains. 6 µl of total lipids were analyzed in each experiment. The solvents used to visualize the indicated lipid species are indicated. The results are representative of at least three biological replicates.

Figure 2. Overexpression of Eis functionally restores PDIM production in the Δ*mbtK* strain **A.** TLC analysis of total lipids from the indicated *M. marinum* strains. The NAT genes in lanes 4-8 were constitutively expressed in the ΔmbtK strain using the mycobacterial optimal strain. 6 µl of total lipids was separated for each strain. The indicated solvents and lipids visualized are indicated. The TLC is representative of at least three biological replicates. **B.** Overlay of the predicted structures for MbtK and Eis NATs. The PDB files used were: https://alphafold.ebi.ac.uk/files/AF-B2HMD6-F1-model_v3.pdb and https://alphafold.ebi.ac.uk/files/AF-B2HM88-F1-model_v3.pdb. The structures were overlaid using PyMOL v.2.4.0. **C**. % amino acid identify of the NATs from panel A. Protein sequences were obtained from Mycobrowser (65), and aligned using Clustal Omega (95). **D.** Clustering by phylogenetic neighbor joining tree without distance corrections, generated based on protein alignments generated by Clustal Omega.

440 **Figure 3. PapA5 is N-terminally acetylated by Eis *in vitro.* A.** Table of peptides from proteins
441 in the PDIM/PGL pathways. B. DTNB assay measuring the production of TNB (412nm) upon the
442 acetylation of the PpsA, PpsE, Mas, Pks15/1 and PapA5 peptides by **B.** WT or inactive MbtK and
443 **C.** the RimI protein from *Salmonella typhimurium* with the S18 N-terminal peptide (ARYFRR).
444 DTNB assays were performed in technical triplicate. The data represent the mean product for-
445 mation from all three experiments. Significance was determined using a Student's t-test between
446 the active and inactive forms of each NAT protein. B.* P=0.0417, **** P<0.0001 C. ** P=0.0096**.**
447 **D.** Flow injection analysis of the N-terminal peptide of PpsE with purified MbtK protein. Left panel:
448 peaks corresponding to the unacetylated N-terminal peptide of PpsE. Right panel: mass range
449 corresponding to the acetylated version. **E.** Flow injection of the N-terminal peptide of PapA5
450 incubated with either purified Eis protein or purified MbtK protein. Top left panel: peaks corre-
451 sponding to unacetylated PapA5. Top right: the acetylated version of PapA5 when incubated with
452 Eis. Bottom left panel: peaks corresponding to unacetylated PapA5, Bottom right panel: the same
453 mass range corresponding to the acetylated version of PapA5. **F.** TLC on total lipids from *M.*
454 *marinum.* 6µl total lipid loaded into each lane, PDIM run 3x consecutively in the solvent indicated,
455 PGLs run once in the solvent indicated. PDIM lipids visualized by phosphomolybdic acid and
456 subsequent charring, PGL lipids visualized by 1% a-naphthol and subsequent charring. The TLC
457 is representative of 3 biological replicates, the remaining 2 are shown in Fig. S9.
458
459 **Figure 4. The requirement of MbtK for mycobacterial pathogenesis can be suppressed by**
460 **constitutive expression of Eis or PapA5. A**. RAW 264.7 cells infected with *M. marinum* strains
461 at an MOI of 5. The data is the average of at least 3 independent infections, each performed in
462 biological triplicate. **** P<0.0001, *** P=0.0001, ** P=0.0218, #### P<0.0001. **B.** *Galleria*
463 *mellonella* infected with the *M. marinum* strains indicated. Larvae were injected with $1x10^7$ bacte-
464 ria into the right hindmost proleg. Larvae were infected in 3 groups of 10, for a total of 30 larvae
465 per strain per infection. Data is representative of at least 3 biological replicates, each performed

466 in technical triplicate. Statistical analysis was performed as in (79). Survival curves were com-
467 pared using a log-rank Mantel-Cox test, $P<0.0001$.
468
469 **Figure 5. Model of Interactions between MbtK, Eis and PDIM biosynthesis.** This study re-
470 vealed that MbtK, likely through siderophore production, is required for the production of PDIM
471 and PGL in *M. marinum.* This requirement was complemented in trans by the addition of Myco-
472 bactin J. Constitutive expression of either Eis, or PapA5 specifically suppressed the loss of
473 PDIM/PGL production in the absence of MbtK, suggesting that the N-terminal acetylation of
474 PapA5 could promote the restoration of PDIM/PGL synthesis in the Δ*mbtK* strain.
475
476 **Table Legend**
477 **Table 1. Table of the *M. marinum* genes with their orthologs from *M. tuberculosis* and their**
478 **commonly used names.**

M. marinum gene	*M. tuberculosis* gene	Name
MMAR_1067	*Rv0730*	
MMAR_1968	*Rv2747*	ArgA
MMAR_4519	*Rv0995*	RimJ
MMAR_1839	*Rv2867c*	Emp1
MMAR_1882	*Rv2851c*	ElaA
MMAR_2463	*Rv1653*	ArgJ
MMAR_0522	*Rv0262c*	Aac
MMAR_1123	*Rv3420c*	RimI
MMAR_4496	*Rv0998*	mPat
MMAR_4889	*Rv0802c*	
MMAR_3205	*Rv2170*	
MMAR_0332	*Rv0133*	
MMAR_1341	*Rv3216*	
MMAR_3740	*Rv2416c*	Eis
MMAR_2836	*Rv3225c*	
MMAR_2615		
MMAR_0151		Eis1
*MMAR_3692**	*Rv1347c*	MbtK
MMAR_2744		

479

480 **References**

481 1. L. Favrot, J. S. Blanchard, O. Vergnolle, Bacterial GCN5-Related N-Acetyltransferases:
482 From Resistance to Regulation. *Biochemistry* **55**, 989-1002 (2016).
483 2. J. Gu *et al.*, Cloning and characterization of NAD-dependent protein deacetylase
484 (Rv1151c) from Mycobacterium tuberculosis. *Biochemistry (Mosc)* **74**, 743-748 (2009).
485 3. J. S. Smith *et al.*, A phylogenetically conserved NAD+-dependent protein deacetylase
486 activity in the Sir2 protein family. *Proc Natl Acad Sci U S A* **97**, 6658-6663 (2000).
487 4. J. Landry *et al.*, The silencing protein SIR2 and its homologs are NAD-dependent protein
488 deacetylases. *Proc Natl Acad Sci U S A* **97**, 5807-5811 (2000).
489 5. C. S. Hwang, A. Shemorry, A. Varshavsky, N-terminal acetylation of cellular proteins
490 creates specific degradation signals. *Science* **327**, 973-977 (2010).
491 6. A. Drazic, L. M. Myklebust, R. Ree, T. Arnesen, The world of protein acetylation. *Biochim*
492 *Biophys Acta* **1864**, 1372-1401 (2016).
493 7. H. Nagai *et al.*, A C-terminal translocation signal required for Dot/Icm-dependent delivery
494 of the Legionella RalF protein to host cells. *Proc Natl Acad Sci U S A* **102**, 826-831 (2005).
495 8. W. M. Holmes, B. K. Mannakee, R. N. Gutenkunst, T. R. Serio, Loss of amino-terminal
496 acetylation suppresses a prion phenotype by modulating global protein folding. *Nat*
497 *Commun* **5**, 4383 (2014).
498 9. D. C. Scott *et al.*, Blocking an N-terminal acetylation-dependent protein interaction inhibits
499 an E3 ligase. *Nat Chem Biol* **13**, 850-857 (2017).
500 10. M. Ventura *et al.*, Nuclear translocation of glyceraldehyde-3-phosphate dehydrogenase is
501 regulated by acetylation. *Int J Biochem Cell Biol* **42**, 1672-1680 (2010).
502 11. R. Ree, S. Varland, T. Arnesen, Spotlight on protein N-terminal acetylation. *Exp Mol Med*
503 **50**, 1-13 (2018).
504 12. R. Koch, [Tuberculosis etiology]. *Dtsch Gesundheitsw* **7**, 457-465 (1884).
505 13. WHO, Global Tuberculosis Report 2023. (2024).
506 14. T. C. Pozos, L. Ramakrishnan, New models for the study of Mycobacterium-host
507 interactions. *Curr Opin Immunol* **16**, 499-505 (2004).
508 15. T. P. Stinear *et al.*, Insights from the complete genome sequence of Mycobacterium
509 marinum on the evolution of Mycobacterium tuberculosis. *Genome Res* **18**, 729-741
510 (2008).
511 16. C. R. Thompson, M. M. Champion, P. A. Champion, Quantitative N-Terminal Footprinting
512 of Pathogenic Mycobacteria Reveals Differential Protein Acetylation. *J Proteome Res* **17**,
513 3246-3258 (2018).
514 17. L. Xie *et al.*, Proteome-wide lysine acetylation profiling of the human pathogen
515 Mycobacterium tuberculosis. *Int J Biochem Cell Biol* **59**, 193-202 (2015).
516 18. F. Liu *et al.*, Acetylome analysis reveals diverse functions of lysine acetylation in
517 Mycobacterium tuberculosis. *Mol Cell Proteomics* **13**, 3352-3366 (2014).
518 19. A. Singhal *et al.*, Systematic Analysis of Mycobacterial Acylation Reveals First Example
519 of Acylation-mediated Regulation of Enzyme Activity of a Bacterial Phosphatase. *J Biol*
520 *Chem* **290**, 26218-26234 (2015).
521 20. X. Wu *et al.*, Differential lysine acetylation profiles of Erwinia amylovora strains revealed
522 by proteomics. *J Proteomics* **79**, 60-71 (2013).
523 21. W. Lee, B. C. VanderVen, S. Walker, D. G. Russell, Novel protein acetyltransferase,
524 Rv2170, modulates carbon and energy metabolism in Mycobacterium tuberculosis.
525 *Scientific reports* **7**, 72 (2017).
526 22. K. B. Arun *et al.*, Acetylation of Isoniazid Is a Novel Mechanism of Isoniazid Resistance in
527 Mycobacterium tuberculosis. *Antimicrob Agents Chemother* **65** (2020).
528 23. S. Nambi, N. Basu, S. S. Visweswariah, cAMP-regulated protein lysine acetylases in
529 mycobacteria. *J Biol Chem* **285**, 24313-24323 (2010).

24. H. Yang *et al.*, Lysine acetylation of DosR regulates the hypoxia response of Mycobacterium tuberculosis. *Emerg Microbes Infect* **7**, 34 (2018).
25. S. Nambi *et al.*, Cyclic AMP-dependent protein lysine acylation in mycobacteria regulates fatty acid and propionate metabolism. *J Biol Chem* **288**, 14114-14124 (2013).
26. K. D. Green *et al.*, Acetylation by Eis and Deacetylation by Rv1151c of Mycobacterium tuberculosis HupB: Biochemical and Structural Insight. *Biochemistry* **57**, 781-790 (2018).
27. K. H. Kim *et al.*, Mycobacterium tuberculosis Eis protein initiates suppression of host immune responses by acetylation of DUSP16/MKP-7. *Proc Natl Acad Sci U S A* **109**, 7729-7734 (2012).
28. M. A. Zaunbrecher, R. D. Sikes, Jr., B. Metchock, T. M. Shinnick, J. E. Posey, Overexpression of the chromosomally encoded aminoglycoside acetyltransferase eis confers kanamycin resistance in Mycobacterium tuberculosis. *Proc Natl Acad Sci U S A* **106**, 20004-20009 (2009).
29. W. Chen, T. Biswas, V. R. Porter, O. V. Tsodikov, S. Garneau-Tsodikova, Unusual regioversatility of acetyltransferase Eis, a cause of drug resistance in XDR-TB. *Proc Natl Acad Sci U S A* **108**, 9804-9808 (2011).
30. D. Pathak, A. H. Bhat, V. Sapehia, J. Rai, A. Rao, Biochemical evidence for relaxed substrate specificity of Nalpha-acetyltransferase (Rv3420c/rimI) of Mycobacterium tuberculosis. *Scientific reports* **6**, 28892 (2016).
31. P. I. Pletnev *et al.*, Ribosomal protein S18 acetyltransferase RimI is responsible for the acetylation of elongation factor Tu. *J Biol Chem* **298**, 101914 (2022).
32. J. A. Armstrong, P. D. Hart, Response of cultured macrophages to Mycobacterium tuberculosis, with observations on fusion of lysosomes with phagosomes. *J Exp Med* **134**, 713-740 (1971).
33. J. A. Armstrong, P. D. Hart, Phagosome-lysosome interactions in cultured macrophages infected with virulent tubercle bacilli. Reversal of the usual nonfusion pattern and observations on bacterial survival. *J Exp Med* **142**, 1-16 (1975).
34. M. A. Fisher, B. B. Plikaytis, T. M. Shinnick, Microarray analysis of the Mycobacterium tuberculosis transcriptional response to the acidic conditions found in phagosomes. *J Bacteriol* **184**, 4025-4032 (2002).
35. K. H. Rohde, R. B. Abramovitch, D. G. Russell, Mycobacterium tuberculosis invasion of macrophages: linking bacterial gene expression to environmental cues. *Cell host & microbe* **2**, 352-364 (2007).
36. T. Hsu *et al.*, The primary mechanism of attenuation of bacillus Calmette-Guerin is a loss of secreted lytic function required for invasion of lung interstitial tissue. *Proc Natl Acad Sci U S A* **100**, 12420-12425 (2003).
37. S. A. Stanley, S. Raghavan, W. W. Hwang, J. S. Cox, Acute infection and macrophage subversion by Mycobacterium tuberculosis require a specialized secretion system. *Proc Natl Acad Sci U S A* **100**, 13001-13006 (2003).
38. P. S. Manzanillo, M. U. Shiloh, D. A. Portnoy, J. S. Cox, Mycobacterium Tuberculosis Activates the DNA-Dependent Cytosolic Surveillance Pathway within Macrophages. *Cell host & microbe* **11**, 469-480 (2012).
39. N. van der Wel *et al.*, M. tuberculosis and M. leprae translocate from the phagolysosome to the cytosol in myeloid cells. *Cell* **129**, 1287-1298 (2007).
40. R. Simeone *et al.*, Phagosomal rupture by Mycobacterium tuberculosis results in toxicity and host cell death. *PLoS Pathog* **8**, e1002507 (2012).
41. J. Quigley *et al.*, The Cell Wall Lipid PDIM Contributes to Phagosomal Escape and Host Cell Exit of Mycobacterium tuberculosis. *MBio* **8** (2017).
42. M. M. Osman, A. J. Pagan, J. K. Shanahan, L. Ramakrishnan, Mycobacterium marinum phthiocerol dimycocerosates enhance macrophage phagosomal permeabilization and membrane damage. *PloS one* **15**, e0233252 (2020).

581 43. J. Augenstreich, V. Briken, Host Cell Targets of Released Lipid and Secreted Protein
582 Effectors of Mycobacterium tuberculosis. *Frontiers in cellular and infection microbiology*
583 **10**, 595029 (2020).
584 44. B. S. Jones *et al.*, The loss of the PDIM/PGL virulence lipids causes differential secretion
585 of ESX-1 substrates in Mycobacterium marinum. *mSphere* **9**, e0000524 (2024).
586 45. A. G. Birhanu *et al.*, N(epsilon)- and O-Acetylation in Mycobacterium tuberculosis Lineage
587 7 and Lineage 4 Strains: Proteins Involved in Bioenergetics, Virulence, and Antimicrobial
588 Resistance Are Acetylated. *J Proteome Res* **16**, 4045-4059 (2017).
589 46. O. A. Collars *et al.*, An N-acetyltransferase required for ESAT-6 N-terminal acetylation and
590 virulence in Mycobacterium marinum. *mBio* **14**, e0098723 (2023).
591 47. J. Augenstreich *et al.*, ESX-1 and phthiocerol dimycocerosates of Mycobacterium
592 tuberculosis act in concert to cause phagosomal rupture and host cell apoptosis. *Cell*
593 *Microbiol* 10.1111/cmi.12726 (2017).
594 48. L. Y. Gao *et al.*, A mycobacterial virulence gene cluster extending RD1 is required for
595 cytolysis, bacterial spreading and ESAT-6 secretion. *Mol Microbiol* **53**, 1677-1693 (2004).
596 49. K. M. Guinn *et al.*, Individual RD1-region genes are required for export of ESAT-6/CFP-
597 10 and for virulence of Mycobacterium tuberculosis. *Mol Microbiol* **51**, 359-370 (2004).
598 50. D. G. Christensen *et al.*, Identification of Novel Protein Lysine Acetyltransferases in
599 Escherichia coli. *MBio* **9** (2018).
600 51. H. Xu, S. S. Hegde, J. S. Blanchard, Reversible acetylation and inactivation of
601 Mycobacterium tuberculosis acetyl-CoA synthetase is dependent on cAMP. *Biochemistry*
602 **50**, 5883-5892 (2011).
603 52. H. J. Lee, P. T. Lang, S. M. Fortune, C. M. Sassetti, T. Alber, Cyclic AMP regulation of
604 protein lysine acetylation in Mycobacterium tuberculosis. *Nat Struct Mol Biol* **19**, 811-818
605 (2012).
606 53. S. Ghosh, B. Padmanabhan, C. Anand, V. Nagaraja, Lysine acetylation of the
607 Mycobacterium tuberculosis HU protein modulates its DNA binding and genome
608 organization. *Mol Microbiol* **100**, 577-588 (2016).
609 54. O. Vergnolle, H. Xu, J. S. Blanchard, Mechanism and regulation of mycobactin fatty acyl-
610 AMP ligase FadD33. *J Biol Chem* **288**, 28116-28125 (2013).
611 55. C. A. Madigan *et al.*, Lipidomic analysis links mycobactin synthase K to iron uptake and
612 virulence in M. tuberculosis. *PLoS Pathog* **11**, e1004792 (2015).
613 56. R. Krithika *et al.*, A genetic locus required for iron acquisition in Mycobacterium
614 tuberculosis. *Proc Natl Acad Sci U S A* **103**, 2069-2074 (2006).
615 57. P. Brodin *et al.*, Dissection of ESAT-6 system 1 of Mycobacterium tuberculosis and impact
616 on immunogenicity and virulence. *Infect Immun* **74**, 88-98 (2006).
617 58. J. Yu *et al.*, Both phthiocerol dimycocerosates and phenolic glycolipids are required for
618 virulence of Mycobacterium marinum. *Infect Immun* **80**, 1381-1389 (2012).
619 59. A. K. Azad, T. D. Sirakova, L. M. Rogers, P. E. Kolattukudy, Targeted replacement of the
620 mycocerosic acid synthase gene in Mycobacterium bovis BCG produces a mutant that
621 lacks mycosides. *Proc Natl Acad Sci U S A* **93**, 4787-4792 (1996).
622 60. A. K. Azad, T. D. Sirakova, N. D. Fernandes, P. E. Kolattukudy, Gene knockout reveals a
623 novel gene cluster for the synthesis of a class of cell wall lipids unique to pathogenic
624 mycobacteria. *J Biol Chem* **272**, 16741-16745 (1997).
625 61. O. A. Trivedi *et al.*, Dissecting the mechanism and assembly of a complex virulence
626 mycobacterial lipid. *Mol Cell* **17**, 631-643 (2005).
627 62. L. R. Camacho *et al.*, Analysis of the phthiocerol dimycocerosate locus of Mycobacterium
628 tuberculosis. Evidence that this lipid is involved in the cell wall permeability barrier. *J Biol*
629 *Chem* **276**, 19845-19854 (2001).
630 63. M. Mathur, P. E. Kolattukudy, Molecular cloning and sequencing of the gene for
631 mycocerosic acid synthase, a novel fatty acid elongating multifunctional enzyme, from

632 Mycobacterium tuberculosis var. bovis Bacillus Calmette-Guerin. *J Biol Chem* **267**, 19388-
633 19395 (1992).
634 64. D. D. Hu, S. D. Weaver, O. A. Collars, P. A. Champion, M. M. Champion, N-terminal
635 proteomics of Mycobacterium marinum using bottom-up label-free quantitative analysis in
636 data-dependent acquisition mode on a timsTOF Pro mass spectrometer. *Microbiol Resour*
637 *Announc* **13**, e0126323 (2024).
638 65. A. Kapopoulou, J. M. Lew, S. T. Cole, The MycoBrowser portal: a comprehensive and
639 manually annotated resource for mycobacterial genomes. *Tuberculosis (Edinburgh,*
640 *Scotland)* **91**, 8-13 (2011).
641 66. S. D. Ley *et al.*, Melting the eis: Nondetection of Kanamycin Resistance Markers by
642 Routine Diagnostic Tests and Identification of New eis Promoter Variants. *Antimicrob*
643 *Agents Chemother* **65**, e0250220 (2021).
644 67. M. B. Gikalo, E. Y. Nosova, L. Y. Krylova, A. M. Moroz, The role of eis mutations in the
645 development of kanamycin resistance in Mycobacterium tuberculosis isolates from the
646 Moscow region. *J Antimicrob Chemother* **67**, 2107-2109 (2012).
647 68. A. Sowajassatakul, T. Prammananan, A. Chaiprasert, S. Phunpruch, Overexpression of
648 eis without a mutation in promoter region of amikacin- and kanamycin-resistant
649 Mycobacterium tuberculosis clinical strain. *Ann Clin Microbiol Antimicrob* **17**, 33 (2018).
650 69. A. Sowajassatakul, T. Prammananan, A. Chaiprasert, S. Phunpruch, Molecular
651 characterization of amikacin, kanamycin and capreomycin resistance in M/XDR-TB strains
652 isolated in Thailand. *BMC Microbiol* **14**, 165 (2014).
653 70. P. Kambli *et al.*, Correlating rrs and eis promoter mutations in clinical isolates of
654 Mycobacterium tuberculosis with phenotypic susceptibility levels to the second-line
655 injectables. *Int J Mycobacteriol* **5**, 1-6 (2016).
656 71. J. Carter, C. R. Consortium, Quantitative measurement of antibiotic resistance in
657 Mycobacterium tuberculosis reveals genetic determinants of resistance and susceptibility
658 in a target gene approach. *Res Sq* 10.21203/rs.3.rs-3378915/v1 (2023).
659 72. M. W. Vetting, D. C. Bareich, M. Yu, J. S. Blanchard, Crystal structure of RimI from
660 Salmonella typhimurium LT2, the GNAT responsible for N(alpha)-acetylation of ribosomal
661 protein S18. *Protein Sci* **17**, 1781-1790 (2008).
662 73. H. Foyn, P. R. Thompson, T. Arnesen, DTNB-Based Quantification of In Vitro Enzymatic
663 N-Terminal Acetyltransferase Activity. *Methods in molecular biology (Clifton, N.J* **1574**, 9-
664 15 (2017).
665 74. A. Yoshikawa, S. Isono, A. Sheback, K. Isono, Cloning and nucleotide sequencing of the
666 genes rimI and rimJ which encode enzymes acetylating ribosomal proteins S18 and S5 of
667 Escherichia coli K12. *Mol Gen Genet* **209**, 481-488 (1987).
668 75. E. Rwegasila, E. B. Mubofu, S. S. Nyandoro, P. Erasto, J. J. Munissi, Preparation,
669 Characterization and in Vivo Antimycobacterial Studies of Panchovillin-Chitosan
670 Nanocomposites. *Int J Mol Sci* **17** (2016).
671 76. M. Meir, T. Grosfeld, D. Barkan, Establishment and Validation of Galleria mellonella as a
672 Novel Model Organism To Study Mycobacterium abscessus Infection, Pathogenesis, and
673 Treatment. *Antimicrob Agents Chemother* **62** (2018).
674 77. Y. Li *et al.*, Galleria mellonella - a novel infection model for the Mycobacterium tuberculosis
675 complex. *Virulence* **9**, 1126-1137 (2018).
676 78. F. M. Entwistle, P. J. Coote, Evaluation of greater wax moth larvae, Galleria mellonella,
677 as a novel in vivo model for non-tuberculosis Mycobacteria infections and antibiotic
678 treatments. *J Med Microbiol* **67**, 585-597 (2018).
679 79. M. Asai *et al.*, Galleria mellonella as an infection model for the virulent Mycobacterium
680 tuberculosis H37Rv. *Virulence* **13**, 1543-1557 (2022).

80. S. S. Chavadi *et al.*, The mycobacterial acyltransferase PapA5 is required for biosynthesis of cell wall-associated phenolic glycolipids. *Microbiology (Reading)* **158**, 1379-1387 (2012).
81. P. Santos-Junior *et al.*, A consensus reverse docking approach for identification of a competitive inhibitor of acetyltransferase enhanced intracellular survival protein from Mycobacterium tuberculosis. *Bioorg Med Chem* **108**, 117774 (2024).
82. L. Radhakrishnan, R. Dani, I. Navabshan, S. Jamal, N. Ahmed, Targeting Aminoglycoside Acetyltransferase Activity of Mycobacterium tuberculosis (H37Rv) Derived Eis (Enhanced Intracellular Survival) Protein with Quercetin. *Protein J* **43**, 12-23 (2024).
83. A. H. Pang, K. D. Green, O. V. Tsodikov, S. Garneau-Tsodikova, Discovery and development of inhibitors of acetyltransferase Eis to combat Mycobacterium tuberculosis. *Methods Enzymol* **690**, 369-396 (2023).
84. S. P. Swain *et al.*, In silico studies of alkaloids and their derivatives against N-acetyltransferase EIS protein from Mycobacterium tuberculosis. *J Biomol Struct Dyn* 10.1080/07391102.2023.2259487, 1-15 (2023).
85. A. H. Pang *et al.*, Discovery and Mechanistic Analysis of Structurally Diverse Inhibitors of Acetyltransferase Eis among FDA-Approved Drugs. *Biochemistry* **62**, 710-721 (2023).
86. A. H. Pang *et al.*, Discovery of substituted benzyloxy-benzylamine inhibitors of acetyltransferase Eis and their anti-mycobacterial activity. *Eur J Med Chem* **242**, 114698 (2022).
87. A. Punetha *et al.*, Structure-based design of haloperidol analogues as inhibitors of acetyltransferase Eis from Mycobacterium tuberculosis to overcome kanamycin resistance. *RSC Med Chem* **12**, 1894-1909 (2021).
88. A. Punetha *et al.*, Structure-Guided Optimization of Inhibitors of Acetyltransferase Eis from Mycobacterium tuberculosis. *ACS chemical biology* **15**, 1581-1594 (2020).
89. K. D. Green, A. Punetha, C. Hou, S. Garneau-Tsodikova, O. V. Tsodikov, Probing the Robustness of Inhibitors of Tuberculosis Aminoglycoside Resistance Enzyme Eis by Mutagenesis. *ACS Infect Dis* **5**, 1772-1778 (2019).
90. H. X. Ngo *et al.*, Potent 1,2,4-Triazino[5,6 b]indole-3-thioether Inhibitors of the Kanamycin Resistance Enzyme Eis from Mycobacterium tuberculosis. *ACS Infect Dis* **4**, 1030-1040 (2018).
91. F. Sanz-Garcia *et al.*, Mycobacterial Aminoglycoside Acetyltransferases: A Little of Drug Resistance, and a Lot of Other Roles. *Frontiers in microbiology* **10**, 46 (2019).
92. P. Knobloch *et al.*, Mycobacterium marinum produces distinct mycobactin and carboxymycobactin siderophores to promote growth in broth and phagocytes. *Cell Microbiol* **22**, e13163 (2020).
93. K. L. Ung, L. Kremer, M. Blaise, Structural analysis of the N-acetyltransferase Eis1 from Mycobacterium abscessus reveals the molecular determinants of its incapacity to modify aminoglycosides. *Proteins* **89**, 94-106 (2021).
94. P. A. Champion, S. A. Stanley, M. M. Champion, E. J. Brown, J. S. Cox, C-terminal signal sequence promotes virulence factor secretion in Mycobacterium tuberculosis. *Science* **313**, 1632-1636 (2006).
95. F. Sievers *et al.*, Fast, scalable generation of high-quality protein multiple sequence alignments using Clustal Omega. *Molecular systems biology* **7**, 539 (2011).

732 Figure 1.

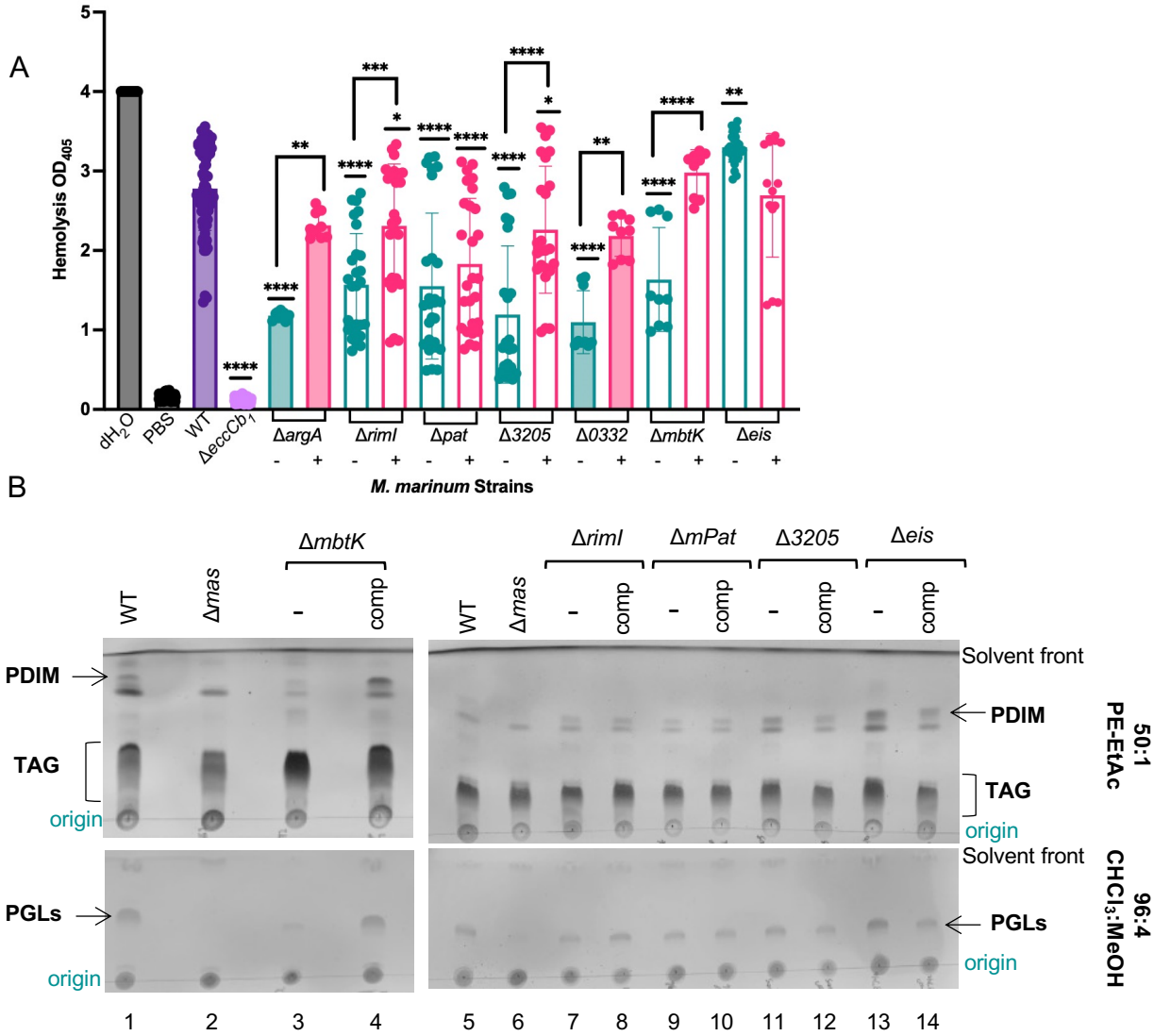

733
734
735

736 Figure 2.

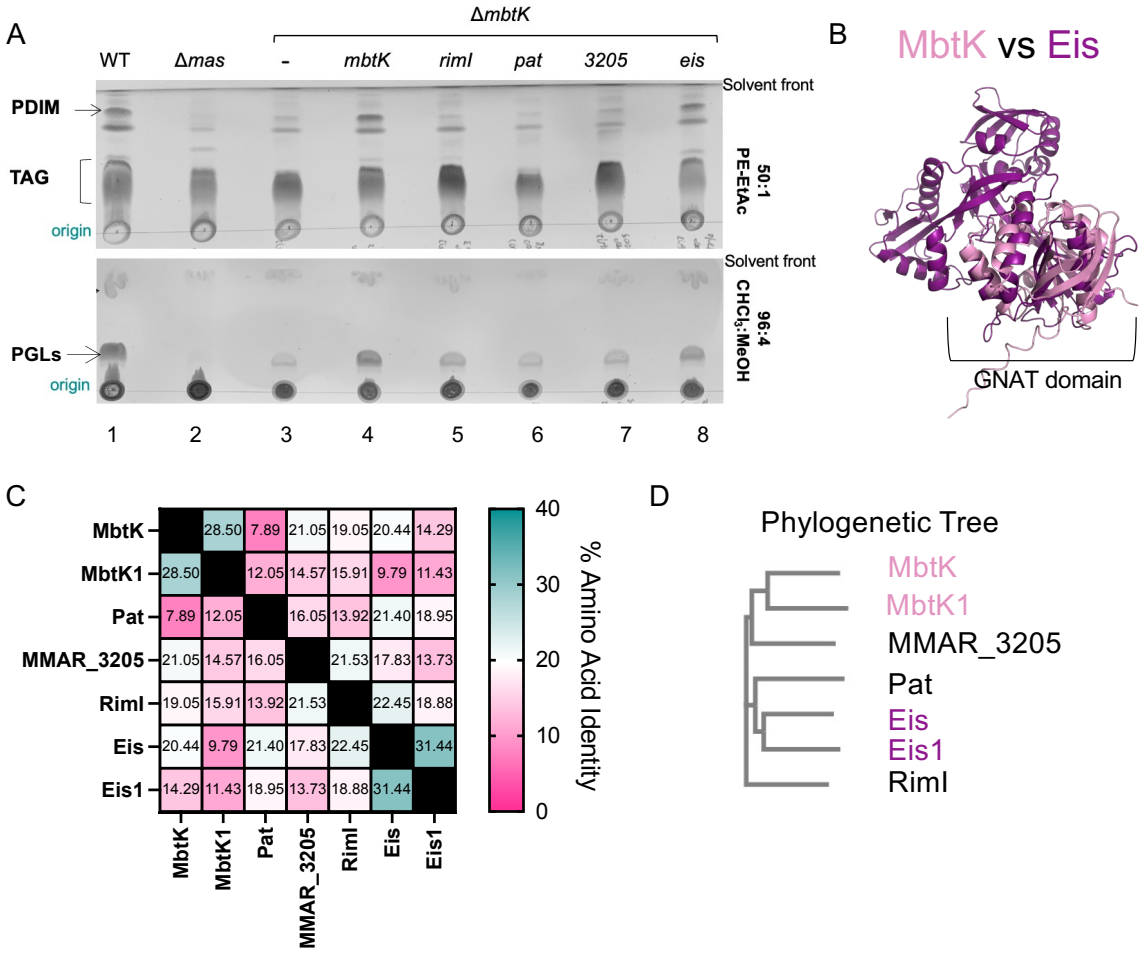

737
738

739 Figure 3.

A

Protein	Nt-Peptide Sequence	Pathway
PpsA	TPSIGG	PGL/PDIM
PpsE	STIPDN	PGL/PDIM
Pks15/1	TTSGES	PGL
Mas	MQKPAT	PGL/PDIM
PapA5	MFPGAV	PGL/PDIM

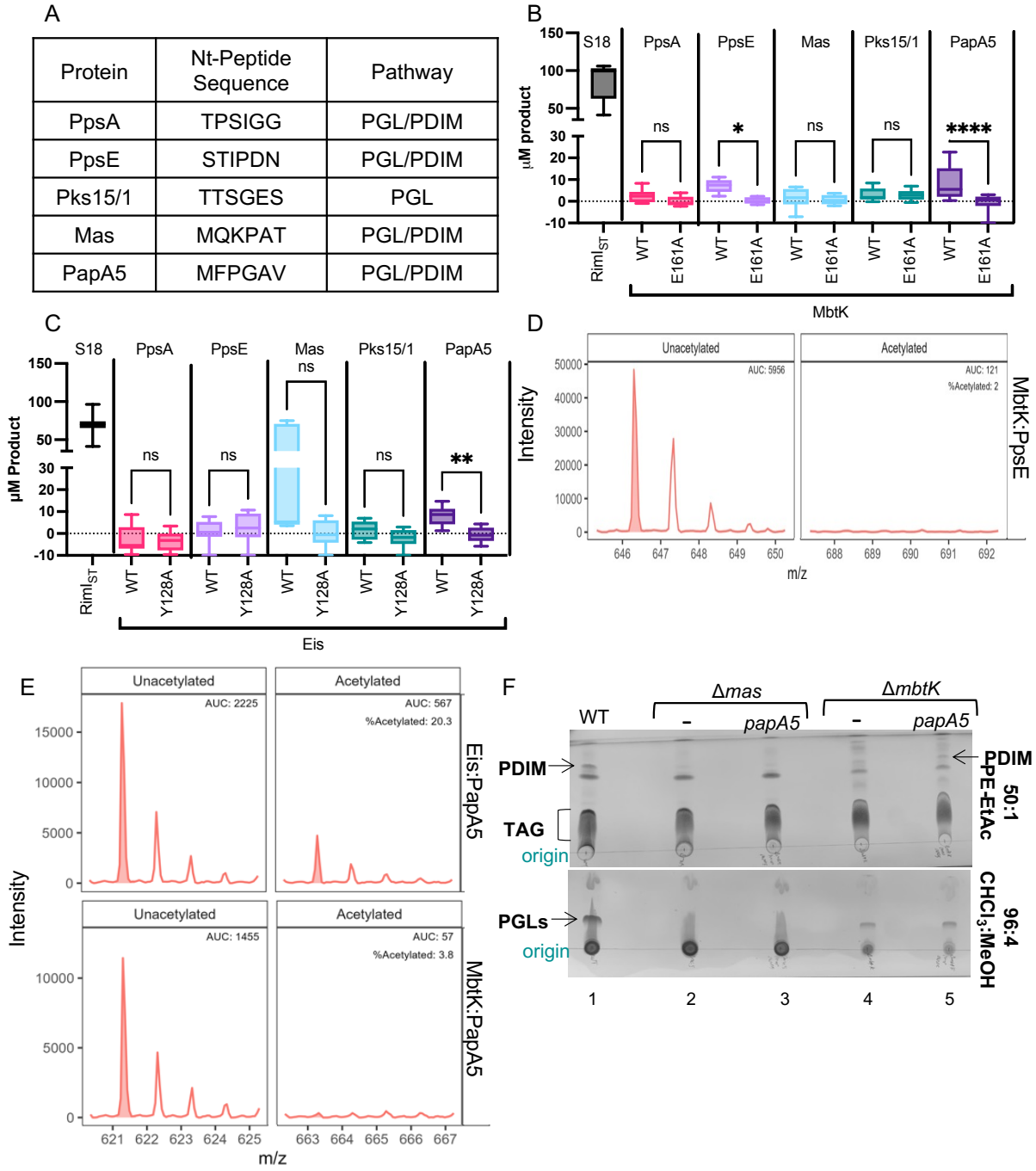

740
741

742 Figure 4.

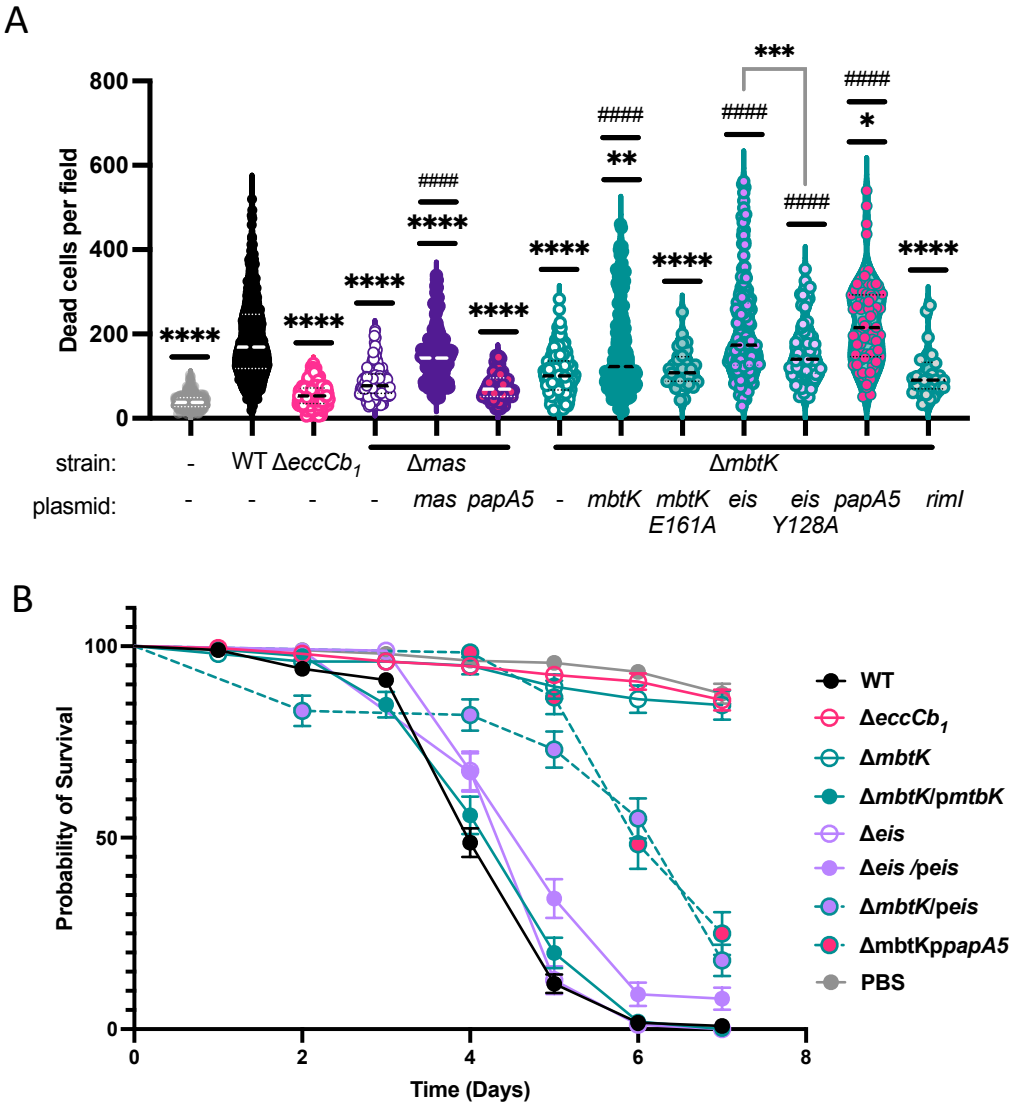

743
744
745

Figure 5.

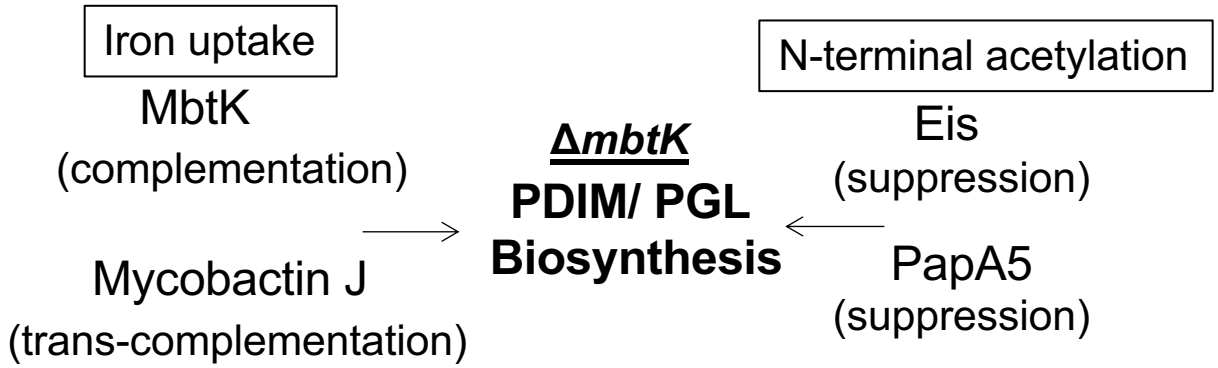
Iron uptake
MbtK
(complementation)
Mycobactin J
(trans-complementation)
ΔmbtK
PDIM/ PGL
Biosynthesis
N-terminal acetylation
Eis
(suppression)
PapA5
(suppression)